

# NEW CONSTRAINTS ON COSMIC POLARIZATION ROTATION FROM B-MODE POLARIZATION IN COSMIC MICROWAVE BACKGROUND

Sperello di Serego Alighieri<sup>1</sup>, Wei-Tou Ni<sup>2</sup> and Wei-Ping Pan<sup>2</sup>

<sup>1</sup>INAF-Osservatorio Astrofisico di Arcetri,  
Largo Enrico Fermi 5, 50125 Firenze, Italy

*E-mail:* [sperello@arcetri.astro.it](mailto:sperello@arcetri.astro.it)

<sup>2</sup>Department of Physics, National Tsing Hua University,  
Hsinchu, Taiwan 30013, Republic of China

*E-mail:* [weitou@gmail.com](mailto:weitou@gmail.com) , [d9722518@oz.nthu.edu.tw](mailto:d9722518@oz.nthu.edu.tw)

## ABSTRACT

The BICEP2 collaboration has recently detected the cosmic microwave background (CMB) B-mode polarization around  $\ell \sim 80$ , with the tensor-to-scalar ratio  $r \approx 0.2$ . We propose two modifications of their analysis of the BB power spectra: 1) include in the model also the effects induced by the cosmic polarization rotation, in addition to the gravitational lensing and the inflationary gravitational waves components, 2) fit also the data available at  $\ell > 500$ , in addition to the BICEP2 data at smaller  $\ell$ . Our fits using BICEP2 and SPTpol data constrain the mean cosmic polarization rotation angle  $\langle\alpha\rangle$  and its fluctuations  $\delta\alpha$  with  $(\eta^2\langle\alpha\rangle^2 + \langle\delta\alpha^2\rangle)^{1/2} < 0.0345$  rad ( $1.97^\circ$ ) where  $(1-\eta)$  is the efficiency in uniform angle de-rotation. The inclusion of polarization rotation in the model changes slightly the tensor-to-scalar ratio ( $r = 0.18 \pm 0.03$ ). This method of constraining the cosmic polarization rotation is new, is complementary to previous tests, which use the radio and optical/UV polarization of radio galaxies and the CMB E-mode polarization, and adds a new constraint for the sky areas observed by SPTpol and BICEP2.

*Key words:* cosmic background radiation – cosmological parameters – early universe – gravitation – inflation – polarization

## 1. INTRODUCTION

The BICEP2 collaboration (Ade et al. 2014b) has recently detected the cosmic microwave background (CMB) B-mode (tensor mode) polarization and finds an excess power around  $\ell \sim 80$  over the gravitational lensing expectation with a significance of more than  $5\sigma$ , which they interpret as due to inflationary gravitational

waves with a tensor-to-scalar ratio  $r = 0.20^{+0.07}_{-0.05}$ . This result is in apparent contrast with the limit previously set by the Planck collaboration  $r < 0.11$  at 95% CL (Ade et al. 2014a). Three processes can produce B-mode polarization: (i) gravitational lensing from E-mode polarization (Zaldarriaga & Seljak 1997), (ii) local quadrupole anisotropies in the CMB within the last scattering region by large scale gravitational waves (Polnarev 1985) and (iii) cosmic polarization rotation (CPR)<sup>1</sup> due to pseudoscalar-photon interaction (Ni 1973; for a review, see Ni 2010). The BICEP2 Collaboration (Ade et al. 2014b) has not considered this latter component in their model. To look for new constraints on the CPR and into the robustness of the BICEP2 fit, we include the CPR effect in the model. TE and TB correlations give mean values of CPR angle  $\langle \alpha \rangle$ , while the contribution of CPR effects to B-mode power gives  $\langle \alpha \rangle^2$  plus the variations of the CPR angle squared  $\langle \delta \alpha^2 \rangle$ . We include in our analysis of the B-mode power spectra also the data available for  $\ell > 500$ , in particular from SPTpol (Hanson et al. 2013) and POLARBEAR (Ade et al. 2014c), in addition those from BICEP2 for smaller  $\ell$ . Our fits give  $r = 0.18 \pm 0.03$  and  $\underline{\alpha}_\eta^2 = \eta^2 \langle \alpha \rangle^2 + \langle \delta \alpha^2 \rangle = 0.000667 \pm 0.00052$ , where  $(1-\eta)$  is the efficiency in the uniform angle de-rotation, which is sometime applied to the measured CMB Q and U maps to compensate for insufficient calibrations of the polarization angle (Keating et al. 2013). This value of  $\underline{\alpha}_\eta^2$  results in an upper limit  $\underline{\alpha}_\eta < 0.0345$  rad ( $1.97^\circ$ ). This method of constraining the CPR is new, is complementary to previous tests, which use the radio and optical/UV polarization of radio galaxies and CMB E-mode polarization (di Serego Alighieri 2011, for a review of these tests), and adds a new constraint for the sky area observed.

In section 2, we review pseudoscalar-photon interaction, its modification on Maxwell equations and the associated electromagnetic propagation effect on polarization rotation. In section 3 we present the results of our fits. In section 4 we review and discuss various constraints on CPR and in section 5 we discuss a few issues and present an outlook towards the future.

## 2. PSEUDOSCALAR-PHOTON INTERACTION, MODIFIED PROPAGATION AND POLARIZATION ROTATION

Einstein Equivalence Principle (EEP) which assumes local special relativity is a major cornerstone of general relativity and metric theories of gravity. Special relativity sprang from Maxwell-Lorentz electrodynamics. Maxwell equations in terms

---

<sup>1</sup> The CPR has also been inappropriately called Cosmological Birefringence, but we follow here the recommendation of Ni (2010).

of field strength  $F_{kl}(\mathbf{E}, \mathbf{B})$  and excitation  $H^{ij}(\mathbf{D}, \mathbf{H})$  do not need metric as primitive concept. Field strength  $F_{kl}(\mathbf{E}, \mathbf{B})$  and excitation  $H^{ij}(\mathbf{D}, \mathbf{H})$  can all be independently defined operationally (e. g. Hehl & Obukhov 2003). To complete this set of equations, one needs the constitutive relation between the excitation and the field in both macroscopic electrodynamics and in space-time theory of gravity:

$$H^{ij} = (1/2) \chi^{ijkl} F_{kl}. \quad (1)$$

When Einstein Equivalence Principle is observed, this fundamental space-time tensor density is induced by the metric  $g^{ij}$  of the form

$$\chi^{ijkl} = (1/2) (-g)^{1/2} (g^{ik} g^{jl} - g^{il} g^{kj}), \quad (g \equiv (\det g^{ij})^{-(1/2)}) \quad (2)$$

and the Maxwell equations can be derived from a Lagrangian density. In local inertial frame, the space-time tensor has the special relativity form  $(1/2) (\eta^{ik} \eta^{jl} - \eta^{il} \eta^{kj})$  with  $\eta^{il}$  the Minkowski metric. To study the empirical foundation of Einstein Equivalence Principle, it is crucial to explore how the experiments/observations constrain the general space-time tensor  $\chi^{ijkl}$  to the GR/metric form.

Since both  $H^{ij}$  and  $F_{kl}$  are antisymmetric,  $\chi^{ijkl}$  must be antisymmetric in  $i$  and  $j$ , and  $k$  and  $l$ . Hence the constitutive tensor density  $\chi^{ijkl}$  has 36 independent components, and can be decomposed to principal part (P), axion part (Ax) and Hehl-Obukhov-Rubilar skewon part (Sk) (Hehl & Obukhov 2003). The skewon  $^{(Sk)}\chi^{ijkl}$  part is antisymmetric in the exchange of index pair  $ij$  and  $kl$ , satisfies a traceless condition, and has 15 independent components. The principal part and the axion (pseudoscalar) part constitute the parts that are symmetric in the exchange of index pair  $ij$  and  $kl$ . Together they have 21 independent components. Axion (pseudoscalar field) part is totally antisymmetric in all 4 indices and can be expressed as  $\varphi e^{ijkl}$  with  $\varphi$  the pseudoscalar field. The principal part then have 20 degrees of freedom.

In constraining the general space-time tensor from experiments and observations, we notice that EEP is already well-tested and can only be violated weakly. Hence, one can start with (2) adding a small general  $^{(Sk)}\chi^{ijkl}$  to look for constraint on skewons first. From the dispersion relation it is shown that no dissipation/no amplification in propagation implies that the additional skewon field must be of Type II (Ni 2014). For Type I skewon field, the dissipation/amplification in propagation is proportional to the frequency and the CMB spectrum would deviate from Planck spectrum. From the high precision agreement of the CMB spectrum to 2.755 K Planck spectrum (Fixsen 2009), the Type I cosmic skewon field  $|^{(SkI)}\chi^{ijkl}|$  is constrained to less than a few parts of  $10^{-35}$  (Ni 2014). Generic Type II skewon field

can be constructed from antisymmetric part of an asymmetric metric and is allowed.

EEP implies that photons with the same initial position and direction follow the same world line independent of energy (frequency) and polarization, i.e. no birefringence and no polarization rotation. This is observed to high precision for no birefringence and constrained for no polarization rotation. Since Type II skewon field in the weak field limit and axion (pseudoscalar) field do not contribute to the dispersion relation in the eikonal approximation (geometrical optics limit), the no-birefringence condition only limits the principal part space-time tensor  ${}^{(P)}\chi^{ijkl}$  to

$${}^{(P)}\chi^{ijkl} = \frac{1}{2} (-h)^{1/2} [h^{ik} h^{jl} - h^{il} h^{kj}] \psi, \quad (3)$$

where the light cone metric  $h^{ik}$  can be expressed in terms of  ${}^{(P)}\chi^{ijkl}$  and Minkowski metric (Ni 1983a, 1984). In the skewonless, the no-birefringence condition is

$$\chi^{ijkl} = \frac{1}{2} (-h)^{1/2} [h^{ik} h^{jl} - h^{il} h^{kj}] \psi + \varphi e^{ijkl}, \quad (4)$$

(Ni 1983a, 1984). Equation (4) has also been proved more recently without weak-field approximation for no-birefringence medium in the skewonless case (Favaro and Bergamin 2011, Lämmerzahl and Hehl 2004). Polarization measurements of electromagnetic waves from pulsars and cosmologically distant astrophysical sources yield stringent constraints agreeing with (4) down to  $2 \times 10^{-32}$  fractionally (for a review Ni 2010).

Constraint of the light cone metric  $h^{il}$  to matter metric  $g^{il}$  up to a scalar factor can be obtained from Hughes-Drever-type experiments and constraint on the dilaton  $\psi$  to 1 (constant) can be obtained from Eötvös-type experiments to high precision (Ni 1983a, 1983b, 1984).

We note that in looking for the empirical foundation of EEP above, only the axion field and Type II skewon field are not well constrained. In Section 4, observational constraints on pseudoscalar-photon interaction (axion field) are reviewed. These give an upper limit of a few degrees for the mean value part of the difference of pseudoscalar field at the last scattering surface and at the observation point. In this paper, we look into further constraint/evidence of pseudoscalar-photon interaction in CMB B-mode polarization, especially on the fluctuation/variation part.

The interaction Lagrangian density for the pseudoscalar-photon interaction is

$$L_1^{(EM-Ax)} = - (1/(16\pi)) \varphi e^{ijkl} F_{ij} F_{kl} = - (1/(4\pi)) \varphi_{,i} e^{ijkl} A_j A_{k,l} \quad (\text{mod div}), \quad (5)$$

where ‘mod div’ means that the two Lagrangian densities are related by integration by

parts in the action integral (Ni 1973, 1974, 1977). If we assume that the  $\varphi$ -term is local CPT invariant, then  $\varphi$  should be a pseudoscalar (function) since  $e^{ijkl}$  is a pseudotensor density. Note that sometimes one inserts a constant parameter to this term; here we absorb this parameter into the definition of the pseudoscalar field  $\varphi$ . The Maxwell equations (Ni 1973, 1977) become

$$F^{ik}{}_{;k} + (-g)^{-1/2} e^{ikml} F_{km} \varphi_{,l} = 0, \quad (6)$$

where the derivation ‘;’ is with respect to the Christoffel connection. The Lorentz force law is the same as in metric theories of gravity or general relativity. Gauge invariance and charge conservation are guaranteed. The modified Maxwell equations (6) are conformal invariant also.

In a local inertial (Lorentz) frame of the  $g$ -metric, (6) is reduced to

$$F^{ik}{}_{,k} + e^{ikml} F_{km} \varphi_{,l} = 0. \quad (7)$$

Analyzing the wave into Fourier components, imposing the radiation gauge condition, and solving the dispersion eigenvalue problem, we obtain  $k = \omega + (n^\mu \varphi_{,\mu} + \varphi_{,0})$  for right circularly polarized wave and  $k = \omega - (n^\mu \varphi_{,\mu} + \varphi_{,0})$  for left circularly polarized wave (Ni 1973; see Ni 2010 for a review). Here  $n^\mu$  is the unit 3-vector in the propagation direction. The group velocity is independent of polarization:

$$v_g = \partial\omega/\partial k = 1. \quad (8)$$

There is no birefringence. This property is well known (Ni 1973, Ni 1984, Hehl and Obukhov 2003, Itin 2013]. For the right circularly polarized electromagnetic wave, the propagation from a point  $P_1$  (4-point) to another point  $P_2$  adds a phase of  $\alpha = \varphi(P_2) - \varphi(P_1)$  to the wave; for left circularly polarized light, the added phase will be opposite in sign (Ni 1973). Linearly polarized electromagnetic wave is a superposition of circularly polarized waves. Its polarization vector will then rotate by an angle  $\alpha$ .

When we integrate along light (wave) trajectory in a global situation, the total polarization rotation (relative to no  $\varphi$ -interaction) is again  $\alpha = \Delta\varphi = \varphi(P_2) - \varphi(P_1)$  for  $\varphi$  is a scalar field where  $\varphi(P_1)$  and  $\varphi(P_2)$  are the values of the scalar field at the beginning and end of the wave. When the propagation distance is over a large part of our observed universe, we call this phenomenon cosmic polarization rotation (Ni 2008).

In the CMB polarization observations, the variations and fluctuations due to pseudoscalar-modified propagation can be expressed as  $\delta\varphi(P_2) - \delta\varphi(P_1)$ , where  $\delta\varphi(P_1)$

is the variation/fluctuation at the last scattering surface.  $\delta\varphi(P_2)$  at the present observation point (fixed) is zero. Therefore the covariance of fluctuation  $\langle[\delta\varphi(P_2) - \delta\varphi(P_1)]^2\rangle$  is the covariance of  $\delta\varphi^2(P_1)$  at the last scattering surface. Since our Universe is isotropic and homogeneous at the last scattering surface to  $\sim 10^{-5}$ , this covariance is  $\sim (\xi \times 10^{-5})^2 \varphi^2(P_1)$  where the parameter  $\xi$  depends on various cosmological models (Ni 2008).

In the propagation, E-mode polarization will rotate into B-mode polarization with  $\sin^2 2\alpha$  ( $\approx 4\alpha^2$  for small  $\alpha$ ) fraction of power. For uniform rotation across the sky, the azimuthal eigenvalue  $\ell$  is invariant under polarization rotation and does not change. For small angle,

$$\alpha = \varphi(P_2) - \varphi(P_1) = [\varphi(P_2) - \varphi(P_1)]_{\text{mean}} + \delta\varphi(P_1), \quad (9)$$

$$\underline{\alpha}^2 \equiv \langle \alpha^2 \rangle = ([\varphi(P_2) - \varphi(P_1)]_{\text{mean}})^2 + \delta\varphi^2(P_1), \quad (10)$$

where  $\underline{\alpha} \equiv \langle \alpha^2 \rangle^{1/2}$  is the root mean-square-sum polarization rotation angle.

In translating the power distribution to azimuthal eigenvalue variable  $\ell$ , we need to insert a factor  $\zeta(\ell) \approx \ell$  in front of  $\delta_l \varphi^2(2)$  to take care of the nonlinear conversion to  $\ell$  due to fluctuations. For uniform rotation with angle  $\alpha$  across the sky, the rotation of (original) E-mode power  $C_l^{EE}$  into B-mode power  $C_l^{BB, \text{obs}}$  is given by (see, e.g., Zhao & Li, 2014):

$$C_l^{BB, \text{obs}} = C_l^{EE} \sin^2(2\alpha). \quad (11)$$

For CPR fluctuation in a patch of sky, the rotated B-mode  $\ell$ -power spectrum  $C_l^{BB, \text{obs}}$  from E-mode power  $C_l^{EE}$  for  $\ell > 30$  and for small CPR angle  $\underline{\alpha}$  is accurately given by

$$C_l^{BB, \text{obs}} \approx C_l^{EE} \sin^2(2\underline{\alpha}) \approx 4\underline{\alpha}^2 C_l^{EE}. \quad (12)$$

This can be shown by comparing the E-mode power spectrum from Figure 10 of Lewis & Challinor (2006) and the B-mode power spectrum from Fig. 5 of Zhao & Li. They are almost identical up to a scale  $4\underline{\alpha}^2$ .

The present BICEP2 data group about 20 azimuthal eigen-modes into one band;  $\zeta(\ell)$  is virtually equal to one. We will set it to  $\ell$  in our analysis. For precise measurement of variations/fluctuations, direct processing of data without first evaluation of the  $\ell$  components may be an alternative method.

### 3. MODELING THE DATA

In this section, we model the available data with the three effects mentioned in the Introduction. The theoretical spectrum of the gravitation-wave tensor B-mode is extracted from Ade et al. (2014b). The polarization-rotated B-mode power spectrum  $C_l^{BB,obs}$ , which we use to fit  $4\alpha^2$  (eq. 12), is obtained from the theoretical E-mode power spectrum  $C_l^{EE}$  of Fig. 10 of Lewis & Challinor (2006). The data on the B-mode power spectrum are the 9 points in Fig. 14 of Ade et al. (2014b) for the low multipole part ( $\ell < 330$ ) and the 4 points in Fig. 2 of Hanson et al. (2013) for  $500 < \ell < 2000$ . The POLARBEAR collaboration has also recently published results for the CMB B-mode polarization for  $500 < \ell < 2100$ , based on observations at 150 GHz on three regions of the sky for a total of 30 deg.<sup>2</sup> (Ade et al. 2014c). However their S/N ratio is considerably lower than the one obtained by the SPTpol collaboration in the same range of  $\ell$ . Therefore we have not considered their data in our fits.

Considering the three contributions to the B-mode, there are two free parameters in the  $\chi^2$  fits:  $r$  (tensor-to-scalar ratio) and  $\alpha_\eta$ , as defined in the Introduction. If the B-mode from the CPR propagation effect due to the pseudoscalar-photon interaction is correlated with the matter distribution, the correlation detection of SPTpol experiment would include this contribution. If that is so, we can further constrain the parameter  $\alpha_\eta$  since the tensor B-mode decreases quickly for  $\ell > 500$ . In our fits we assume 0%, 16.7%, 42.5%, and 100% correlation of the contribution from the cosmic polarization rotation to the power spectra. The fit for 0% correlation is shown in Figure 1 with the E-mode power spectrum shown. This 0% fit is equivalent to a fit which uses only the BICEP2 data, since in the multipole range of SPTpol the contribution of tensor mode is negligible. The fits for 16.7%, 42.5%, and 100% correlation are shown in Figure 2. Figure 3 shows the best-fit values and the diagonal errors for the fits. The dependence of  $\alpha_\eta^2$ ,  $r$ , and  $\chi^2$  on the CPR-SPTpol correlation percentage are shown in Fig. 4.

### 4. CONSTRAINTS ON COSMIC POLARIZATION ROTATION

The CPR has not yet been detected. Upper limits have been obtained from radio galaxies polarization, both in the radio and in the optical/UV (di Serego Alighieri et al. 2010), and from CMB polarization anisotropies. These limits have been reviewed by di Serego Alighieri (2011): all methods have reached an accuracy of about 1° and 3σ upper limits to any rotation of a few degrees. Since this review only minor revisions of the limits from the CMB have appeared (see Table 1). Gluscevic et al. (2012) have

searched for direction-dependent CPR with WMAP 7-year data and obtain an upper limit on the rms rotation angle  $\langle\alpha^2\rangle^{1/2}<9.5^\circ$  for  $0<\ell<512$  and an upper limit at 68% CL of about  $1^\circ$  on the quadrupole of a scale-independent rotation-angle power spectrum.

Table 1: Recent constraints on uniform CPR angle from CMB polarization

Experiment	Frequency	Multipoles	CPR angle	Reference
WMAP9	41,61,94 GHz	2-800	$-0.36^\circ\pm 1.24^\circ\pm 1.5^\circ$	Hinshaw et al 2012
BICEP1	100,150 GHz	20-335	$-2.77^\circ\pm 0.86^\circ\pm 1.3^\circ$	Kaufman et al 2014

The rotation angle given by the revision of BICEP1 data by Kaufman et al. (2014) formally corresponds to a 1.78 sigma detection of CPR. However, taking into account the uncertainties involved in the calibration of the BICEP1 polarization angle, the problems in correcting for galactic Faraday rotation, (Section VI.B of Kaufman et al. 2014), and the inconsistency of this result with the one of QUaD, for which Brown et al. (2009) give a CPR angle of  $0.64^\circ\pm 0.5^\circ(\text{stat.})\pm 0.5^\circ(\text{syst.})$ , we do not consider this CPR “detection” as final. Recently Gubitosi and Paci (2013) have reviewed the constraints on CPR, but they have considered only those deriving from CMB polarization data.

By modeling the BICEP2 and SPTpol data on the B-mode polarization power spectrum taking into account the inflationary gravitational waves, the gravitational lensing, and the component induced by CPR, as explained in the previous sections, we can derive a new constraint on CPR, since our models limit  $\underline{\alpha}_\eta^2 (= \eta^2\langle\alpha^2\rangle + \langle\delta\alpha^2\rangle)$ . In fact in our case, since we cannot predict which should be the correlation percentage between lensing E-mode and B-mode CPR effects, the most conservative CPR constraint is set at the percentage which gives the maximum  $\underline{\alpha}_\eta^2$ , i.e. 16.7% (Fig. 4 top). In fact, we could not consider instead the correlation percentage giving the lowest  $\chi^2$ , i.e. 42.5% (Fig. 4 bottom), also because all correlation percentages between 10% and 100% give  $\chi^2$  values within 10% of the best one, hence they all are statistically acceptable. At 16.7%,  $\underline{\alpha}_\eta^2 = 0.000667\pm 0.000476$ . Therefore we can set a limit:  $(\underline{\alpha}_\eta^2)^{1/2}\leq 0.0345 \text{ rad.} = 1.97^\circ$ , at 68% C.L. We stress that this limit concerns the value  $|\eta\alpha|$  of the modulus of any CPR rotation, eventually corrected for any de-rotation applied to the polarization data, if the rotation is uniform over the whole sky (or rather over the BICEP2 and SPTpol sky areas), or, in case of no uniformity, the rms average of the uniform CPR component and of its fluctuations over the sky area observed by SPTpol.

The new upper limit to CPR angle, which we derive here from the limits on the pseudoscalar effect on the B-mode CMB spectrum ( $|\eta\alpha|\leq 1.97^\circ$ ), is consistent with the

previous tests in not detecting any CPR and has a similar accuracy. It is important because it is specific for the sky area observed, in particular by the SPTpol collaboration (a  $100 \text{ deg}^2$  region with  $23\text{h}<\text{R.A.}<24\text{h}$  and  $-60^\circ<\text{Dec.}<-50^\circ$ , Hanson et al. 2013), since their data at  $\ell>500$  are the most useful data in constraining the CPR component of the BB spectrum (Fig. 2).

There were no previous CPR upper limits specific for this southern region, since there are no polarized radio galaxies in it (di Serego Alighieri et al. 2010). There are also no polarized radio galaxies within the regions of the sky observed by the POLARBEAR collaboration to study the gravitational lensing effect on the B-mode power spectrum of the CMB polarization (Ade et al. 2014c). Actually, out of the 8 polarized radio galaxies which have been considered for the CPR test (di Serego Alighieri et al. 2010), the closest one to a POLARBEAR field is TXS1243+036, which is at  $13.72^\circ$  from the center of their  $3^\circ\times 3^\circ$  field centered at RA=11h53m, Dec.=-0.5°, therefore more than  $10^\circ$  out of this field. The constraint on CPR obtained from TXS1243+036 is  $-12.8^\circ<\alpha<4.8^\circ$  at 68% CL, not particularly stringent.

Our models give a value for  $r$  which is slightly lower than the value given by the BICEP2 collaboration (Ade et al. 2014b), but still in disagreement with the Planck 6-parameter-fit limit (Ade et al. 2014a). However the Planck limit is relaxed to  $r<0.26$  when running is allowed with  $dn_s/d\ln k = -0.022\pm 0.010$  (Ade et al. 2014b). Our fitted  $r$ -value gives a  $6\sigma$  detection, which agrees with the BICEP2 results and shows robustness to adding CPR effects.

Lee et al. (2014) have recently modeled the power spectrum of the B-mode CMB polarization, including a component deriving from CPR (they call it “cosmological birefringence”), therefore decreasing the “primordial” component and bring it within the limit  $r<0.11$  set by Ade et al. (2014a). However they have considered only the BICEP2 data (Ade et al. 2014b) at low  $\ell$ , not the SPTpol data (Hanson et al. 2014) at high  $\ell$ , which together better constrain the CPR. Therefore they allow for a CPR component much larger than we do, considering also the SPTpol data. We believe that our approach is a considerable improvement.

## 5. DISCUSSION AND OUTLOOK

In this paper we have investigated, both theoretically and experimentally, the possibility to detect CPR, or set new constraints to it, using its coupling with the B-mode power spectra of the CMB. Three experiments have detected B-mode polarization in the CMB: SPTpol (Hanson et al. 2013) for  $500<\ell<2700$ , BICEP2 (Ade et al. 2014b) for  $20<\ell<340$ , and POLARBEAR (Ade et al. 2014c) for  $500<\ell<2100$ .

The practical realization of our suggestion has two issues. First, in order to eliminate the observed excess of TB and EB power over the lensing expectations, the BICEP2 and the POLARBEAR collaborations have applied a de-rotation of  $\sim 1^\circ$  to the final Q/U maps by minimizing the TB and EB power, since they cannot calibrate the overall polarization angle at this level of accuracy (Kaufman et al. 2014). By minimizing the TB power, the mean pseudoscalar polarization rotation angle is de-rotated by  $2\alpha$  and only the fluctuation part remains included in the BB polarization spectra. Minimizing EB power, the mean pseudoscalar polarization rotation angle is also de-rotated by about  $2\alpha$ . So the constraint on  $\alpha$  is on the fluctuations and the leftover  $\alpha$  of  $\varphi$  to the precision of rotation. On the other hand the SPTpol collaboration have not explicitly de-rotated their polarization data, but state that, although they have corrected for leakage of the CMB temperature into polarization ( $I \rightarrow Q$  and  $U$ ), the effect of this correction on the measured polarization amplitude is less than  $0.1\sigma$  (Hanson et al. 2013). They also state that their systematic uncertainty on the polarization angle is less than  $1^\circ$  at 150 GHz.

The second practical issue is related to the possible contamination of B-mode power spectra due to foreground anisotropies: the galactic ones are minimized by a careful selection of the observed sky regions, while those due to distant FIR-luminous galaxies can have an effect at  $\ell > 500$  (e.g. Holder et al. 2013). However, the SPTpol team has applied a correction derived from Herschel data (Hanson et al. 2013). On the other hand the POLARBEAR collaboration finds that the foreground contamination is negligible and have not corrected for it (Ade et al. 2014c). We notice that the POLARBEAR data on  $C^{BB}$  at  $\ell=700$  (the only one with  $S/N > 1.5$ ), which is not corrected for foreground contamination, is consistent with the higher  $S/N$  SPTpol data, which have been corrected, giving us some confidence that the correction should not have an adverse influence.

Concerning the prospects for improvements in the detection/constraints on CPR in the near future, the Planck satellite (<http://www.rssd.esa.int/index.php?project=Planck>) is expected to allow for a considerable step forward, since it will have a sensitivity to polarization rotation of the order of a tenth of a degree and systematic errors of the same order (Gruppuso et al. 2012), provided that calibration procedures of sufficient accuracy for the polarization orientation are implemented. In any case the Planck polarization results are foreseen only towards the end of this year. Also the Keck Array, which is a set of 5 telescopes very similar to the BICEP2 one, is expected to bring considerable improvements on current CMB polarization measurements. Three of these telescopes are already operating and results are expected soon, particularly for B-mode polarization due to inflationary gravitational waves (Pryke et al. 2013).

As far as we are aware, there is no current plan for extending the optical/UV polarization measurement of distant radio galaxies to a level which would bring considerable improvements on the CPR constraints obtained so far from these objects. However it would be desirable to perform detailed 2D observations of the optical/UV polarization of a few radio galaxies, of the kind performed on 3C 265 (Wardle, Perley & Cohen 1997) and selected in the sky areas also observed by CMB polarization experiments on the ground. In fact these observations are likely to constrain the CPR angle with an accuracy of better than  $1^\circ$ , thereby providing a better calibration for the absolute polarization angle than available so far to these experiments.

If pseudoscalar-photon interaction exists, a natural cosmic variation of the pseudoscalar field at the decoupling era is  $10^{-5}$  fractionally. The CPR fluctuation is then of the order of  $10^{-5}\phi_{\text{decoupling-era}}$ . We will look for its possibility of detection or more constraints in future experiments.

### Acknowledgements

We thank Brian Keating for useful comments. One of us (WTN) would also like to thank the National Science Council (Grants No. NSC101-2112-M-007-007 and No. NSC102-2112-M-007-019) and the National Center for Theoretical Sciences (NCTS) for supporting this work in part.

### REFERENCES

- Ade, P.A.R. et al. (Planck Collaboration) 2014a, A&A, in press, also arXiv:1303.5076  
Ade, P.A.R. et al. (BICEP2 Collaboration) 2014b, arXiv:1403.3985  
Ade, P.A.R. et al. (Polarbear Collaboration) 2014c, arXiv:1403.2369  
Brown, M.L. et al. (QUaD Collaboration) 2009, ApJ 705, 978  
di Serego Alighieri, S., Finelli, F. & Galaverni, M. 2010, ApJ 715, 33  
di Serego Alighieri, S. 2011, in *From Varying Couplings to Fundamental Physics*, C. Martins and P. Molaro (eds.), ASSP, Springer, p. 139, also arXiv:1011.4865  
Favaro, A. & Bergamin, L. 2011, Annalen der Physik 523, 383  
Fixsen, D. J. 2009, Ap. J. 707, 916  
Gluscevic, V., Hanson, D., Kamionkowski, M. & Hirata, C.M. 2012, Phys. Rev. D 86, 103529  
Gruppuso, A., Natoli, P., Mandolesi, N., De Rosa, A., Finelli, F. & Paci, F. 2012, JCAP 2, 23  
Gubitosi, G. & Paci, F. 2013, JCAP 2, 20  
Hanson, D. et al. (SPTpole Collaboration) 2013, Phys. Rev. Lett. 111, 141301  
Hehl, F.W., Yu, N., and Obukhov, G.F. 2003, *Foundations of Classical*

- Electrodynamics: Charge, Flux, and Metric* (Birkhäuser: Boston, MA)
- Hinshaw, G. et al. (WMAP Collaboration) 2013, ApJS 208, 19
- Holder, G.P. et al. (SPT Collaboration) 2013, ApJL, 771, L16
- Itin, Y. 2013, Phys. Rev. D, 88, 107502
- Komatsu, E. et al. (WMAP Collaboration) 2011, ApJS 192, 18
- Kaufman, J.P. et al. (BICEP1 Collaboration) 2014, Phys. Rev. D 89, 062006
- Keating, B.G., Shimon, M. & Yadav, A.P.S. 2013, ApJL, 762, L23
- Lämmerzahl, C. & Hehl, F.W. 2004, Phys. Rev. D, 70, 105022
- Lee, S., Liu, G.-C. & Ng, K.-W. 2014, arXiv:1403.5585
- Lewis, A. & Challinor, A. 2006, Phys. Rept., 429, 1
- Ni, W.-T. 1973, A Nonmetric Theory of Gravity, Montana State University, <http://astrod.wikispaces.com/>
- Ni, W.-T. 1974, Bull. Am. Phys. Soc., 19, 655
- Ni, W.-T. 1977, Phys. Rev. Lett., 38, 301
- Ni, W.-T. 1983a, in *Proceedings of the 1983 International School and Symposium on Precision Measurement and Gravity Experiment*, ed. W.-T. Ni, (National Tsing Hua University, Hsinchu, Taiwan, Republic of China), 491, <http://astrod.wikispaces.com/>
- Ni, W.-T. 1983b, in *Proceedings of the 1983 International School and Symposium on Precision Measurement and Gravity Experiment*, ed. W.-T. Ni (National Tsing Hua University, Hsinchu, Taiwan, Republic of China), 519, <http://astrod.wikispaces.com/>
- Ni, W.-T. 1984, in *Precision Measurement and Fundamental Constants II*, ed. B. N. Taylor & W. D. Phillips, Natl. Bur. Stand. Spec. Publ. 617, 647
- Ni, W.-T. 2008, *Prog. Theor. Phys. Suppl.*, 172, 49
- Ni, W.-T. 2010, *Reports on Progress in Physics*, 73, 056901
- Ni, W.-T. 2014, Phys. Lett. A 378, 1217
- Polnarev, A. G. 1985, SvA 29, 607
- Pryke, C. et al. (BICEP2 and Keck-Array Collaborations) 2013, in *Astrophysics from Antartica*, IAU Symp. S288, Proc. of the IAU, Vol. 8, p. 68
- Wardle, J.F.C., Perley, R.A. & Cohen, M.H. 1997, Phys. Rev. Lett. 79, 1801
- Zaldarriaga, M. & Seljak, U. 1997, Phys. Rev. D, 55, 18309
- Zhao, W., & Li, M. 2014, arXiv1403.3997

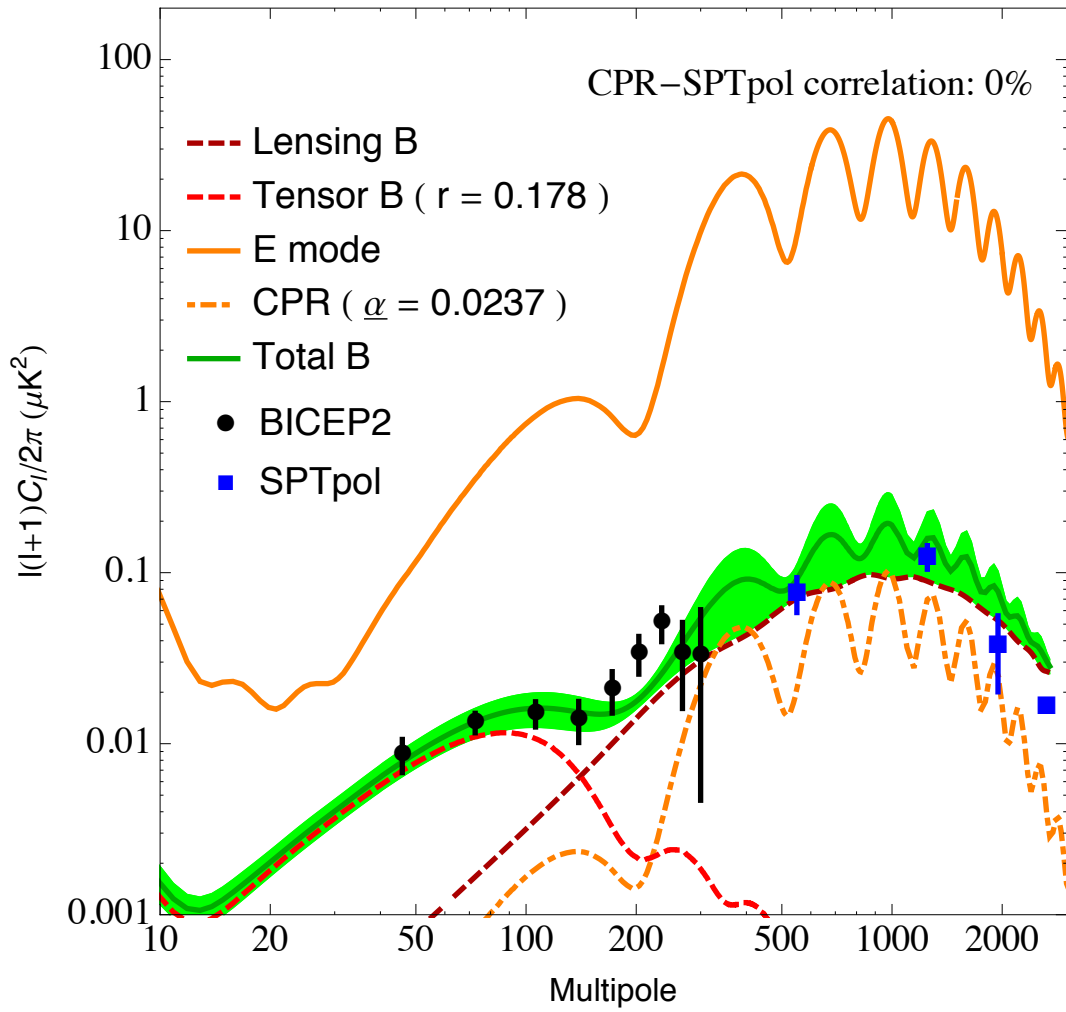


**Figure 1.** The B-mode spectrum showing the best fit (dark green line) and the one  $\sigma$  region (green band) to the BICEP2 (black filled circles) and SPTpol data (blue filled squares) with the vertical bar showing standard deviation of each data point for a 0% correlation. The E-mode is plotted for reference.

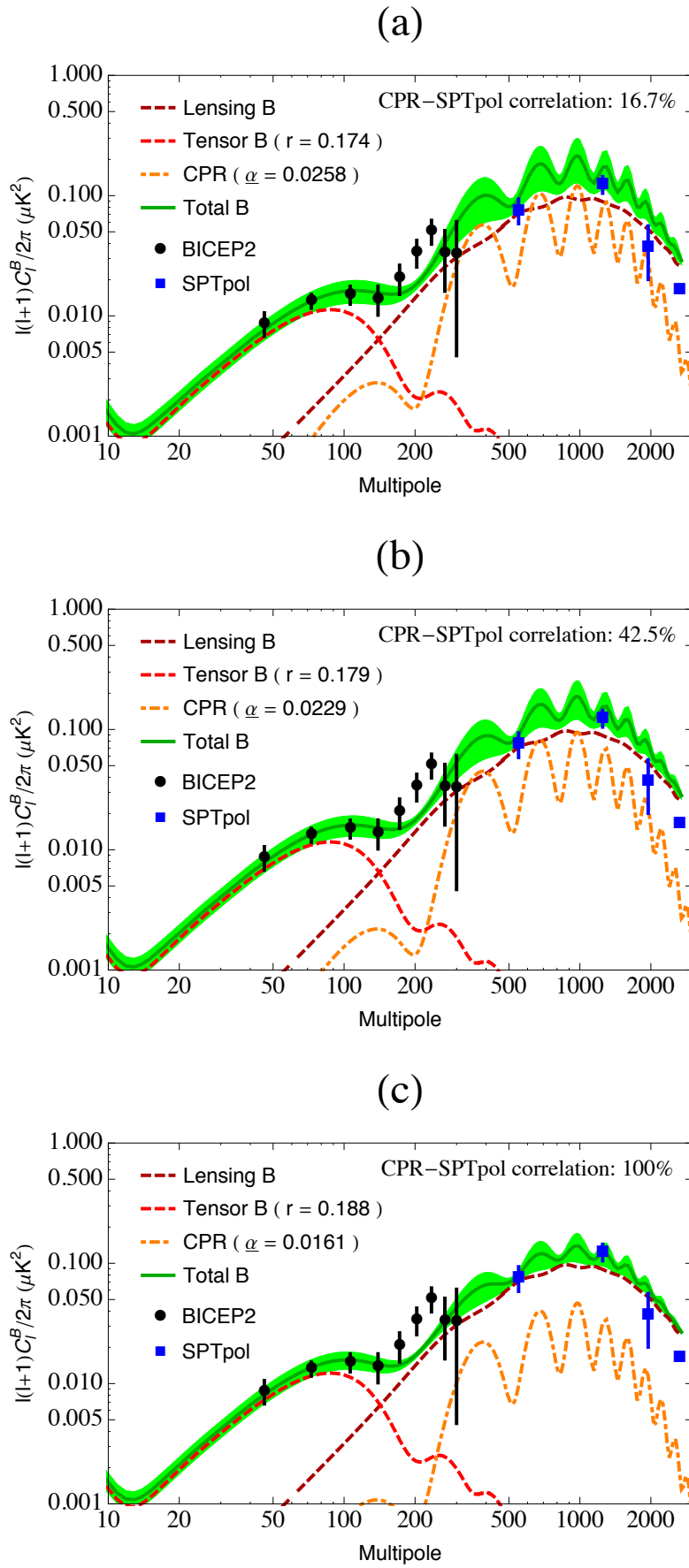
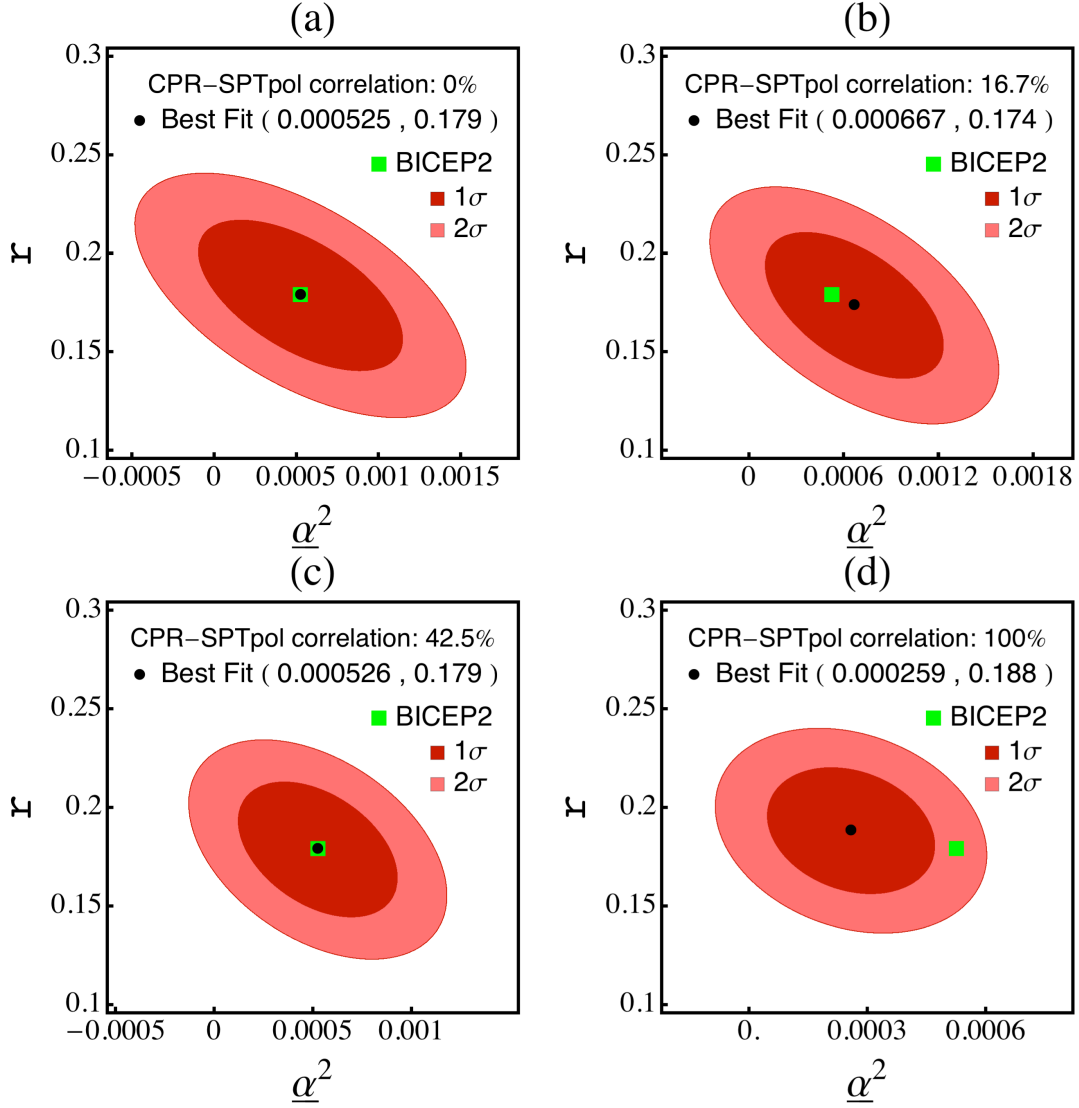


Figure 2. Same as Figure 1, but for 16.7%, 42.5%, and 100% correlation.



**Figure 3.** Joint constraint on the tensor-to-scalar ratio  $r$  and the root-mean-square-sum of CPR angle due to pseudoscalar-photon interaction. 1 $\sigma$  and 2 $\sigma$  contours are shown.

The best fit and diagonal errors of each plot are

(a)  $r_{0\%} = 0.179 \pm 0.031$  and  $\alpha_{0\%}^2 = 0.000525 \pm 0.000508$  ( $\chi^2_{\min}=14.69$ )

(b)  $r_{16.7\%} = 0.174 \pm 0.031$  and  $\alpha_{16.7\%}^2 = 0.000667 \pm 0.000476$  ( $\chi^2_{\min}=13.14$ )

(c)  $r_{42.5\%} = 0.179 \pm 0.031$  and  $\alpha_{42.5\%}^2 = 0.000526 \pm 0.000368$  ( $\chi^2_{\min}=12.46$ )

(d)  $r_{100\%} = 0.188 \pm 0.031$  and  $\alpha_{100\%}^2 = 0.000259 \pm 0.000207$  ( $\chi^2_{\min}=12.93$ )

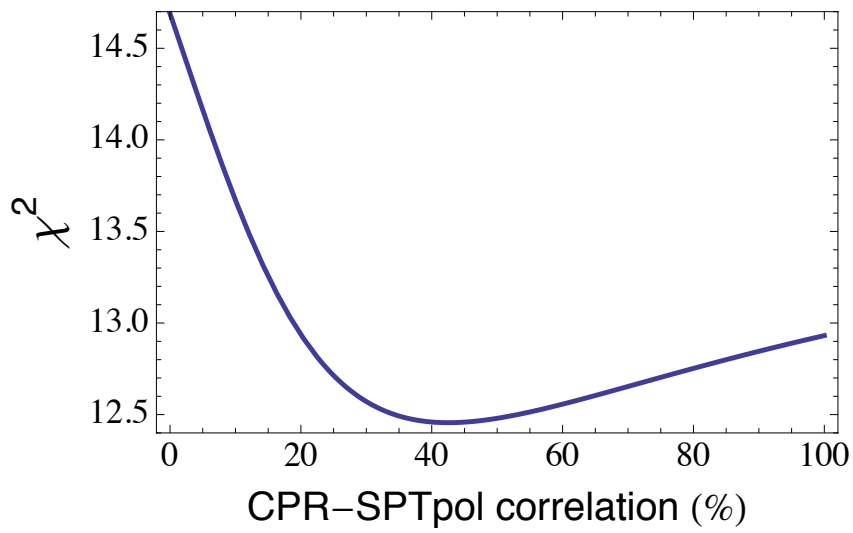
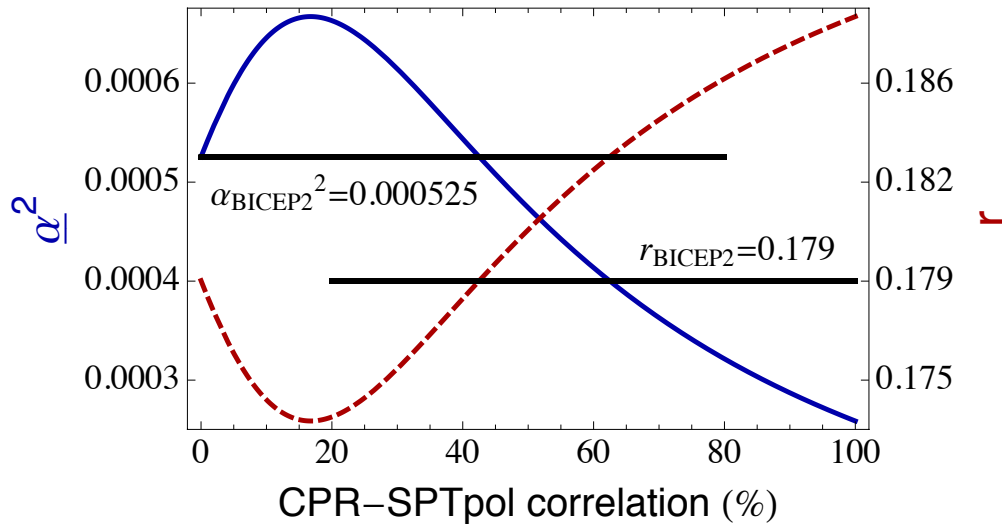


**Figure 4.** The dependence of  $\alpha_1^2$ ,  $r$ , and  $\chi^2$  on the CPR-SPTpol correlation.